

# The Effect of Wick Permeability and Porous Radius on Capillary and Entrainment Limit in A Heat Pipe Reactor

Gizem Bakır 

 Sivas Cumhuriyet University, Department of Manufacturing Engineering, Sivas, Türkiye

## ABSTRACT

For heat extraction in nuclear systems, interest in the design of nuclear reactors with heat pipes has increased. The determination of heat limitations is one of the remarkable factors for safety when heat pipes are used for nuclear systems. In this study, capillary and entrainment limit values for the heat pipe were calculated in a heat pipe reactor with potassium working fluid operating at 650 K. Five different effective porous radii ( $10.1 \times 10^{-6}$ ,  $10.225 \times 10^{-6}$ ,  $10.35 \times 10^{-6}$ ,  $10.425 \times 10^{-6}$  and  $10.6 \times 10^{-6}$  m) and five different wick permeability ( $4.75 \times 10^{-12}$ ,  $5 \times 10^{-12}$ ,  $5.25 \times 10^{-11}$ ,  $5.5 \times 10^{-12}$  and  $5.75 \times 10^{-12}$  m<sup>2</sup>) is considered for sintered copper wick heat pipe. While the effects of effective porosity radius, wick permeability, and wick radius on the capillary barrier were studied, only the effects of effective porosity radius were studied. While the effects of effective porosity radius, wick permeability, and wick radius on the capillary barrier are studied, only the effects of effective porosity radius are studied. The highest values of the capillary and entrainment limits are obtained when the porosity radius is  $10.1 \times 10^{-6}$  m. Besides, maximum capillary limits are achieved when the wick permeability is  $5.75 \times 10^{-12}$  m<sup>2</sup> and the effective porosity radius is  $10.1 \times 10^{-6}$ . This study aims to determine the optimum effective porous radius and wick permeability for this reactor and investigate the effect of effective porous radius and wick permeability on the heat pipe limitations.

### Keywords:

Heat pipe; Nuclear reactor; Porous radius; Wick permeability; Wick radius; Capillary limit; Entrainment limit

## INTRODUCTION

The heat-pipe-cooled reactor stands out with its high-power density, ease of handling, long-term life (>5 years), and reliability. Recently, the investigation of heat pipes for heat transfer in nuclear cores has been a research topic for researchers [1-4]. The heat pipe is a highly efficient and passive heat transfer mechanism that uses latent heat from evaporation without pump power. It is used in many fields, including nuclear reactors, due to its high efficiency. There are some limitations to the heat transfer of heat pipes. Incorrect determination of heat transfer limits may result in calculating the heat extraction values of the heat pipes incorrectly, in this case, thus causing accidents. The capillary limit is one of the most significant limits for determining these limitations.

Heat pipe reactors have become a popular topic due to the efficiency of heat pipes and their increasing area of applications. Sun et al [5] designed a 120 kW lithium heat pipe reactor power supply that can be used for multiple applications. In their design, 70% enriched uranium nitride fuel and lithium heat pipes were used.

For their study, an MCORE code combining MCNP and ORIGEN was used. In general, it was found that the designed basic parameters met the safety requirements, and the reactor was safe in terms of neutronics. Zhang et al. [6], designed a fast reactor that transfers heat to potassium-filled high-temperature pipes and thermoelectric generators. Both finite element and thermal resistance network methods were used to simulate the potassium heat pipe system. The normal operating conditions and two accident scenarios were calculated to prove the reliability of the new system model. Liu et al. [7], proposed the design of a new passive heat removal system using heat pipe technology to develop the passive safety feature of the molten salt reactor. An experimental system was developed to validate the design of the passive heat removal system of the reactor. An eutectic salt mixture was chosen as the working fluid, and different ranges of it were considered for the heat pipes. They reached lower temperatures when they had a greater distance between the heat pipe spacings. The distance between heat pipe spacings was an important factor affecting the temperature difference. Wang et al.

### Article History:

Received: 2023/01/30

Accepted: 2023/10/24

Online: 2023/12/31

Correspondence to: Gizem Bakır,  
E-Mail: [gbakir@cumhuriyet.edu.tr](mailto:gbakir@cumhuriyet.edu.tr)  
Phone: +90 346 487 00 00/2338

This article has been checked for similarity.



This is an open access article under the CC-BY-NC licence

<http://creativecommons.org/licenses/by-nc/4.0/>

### Cite as:

Bakır G, "The effect of wick permeability and porous radius on capillary and entrainment limit in a heat pipe reactor". Hittite J Sci Eng. 2023;10 (4): 279-285. doi:10.17350/hjse19030000317

[8], analyzed a molten salt reactor using high-temperature heat pipe technology. In their study, they set up an experimental system to verify the feasibility of the passive heat extraction system in the reactor. The experimental results showed that although some of the heat pipes did not work normally, the heat pipe system removed a significant amount of heat from the drain tank. Wang et al. [9], investigated the design of a 25 kWe heat pipe cooled reactor for multiple uses. Based upon the heat pipe cooled reactor design, a thermohydraulic computer code was developed to analyze the time-dependent and time-independent performance of the reactor. For this reactor, 65% enriched UN and potassium are used as fuel and heat pipe working fluid, respectively. In their results, the selected parameters met the safety requirements. Guillen and Turner [10] used axially grooved heat pipes and investigated the applicability of these heat pipes for heat extraction in microreactors. The HTPIPE code is used for the analysis. The performance limits of a sodium heat pipe with a threaded square wick structure were compared to those of an equivalent heat pipe with a circular wick. It was reported that, at operating temperatures below 777 °C the annular wick outperforms the corrugated wick, while at temperatures above 777 °C the corrugated wick outperforms the annular wick.

Some researchers have studied the capillary limit in the heat pipe. Subedi et al. [11] studied the thermal properties of a flat micro heat pipe. They calculated the capillary and maximum temperature limits to determine the maximum heat transfer. For the theoretical results of the optimized wick design, the maximum heat transfer rate and the surface temperature distribution were compared for the capillary limit and maximum temperature limit cases. Yu et al. [12] analyzed the effect of the wick geometry of a heat pipe on the heat transfer capacities. A special analytical computer model was designed using the Newton-Raphson method and applied this model to analyze the capillary, viscous, entrainment, sonic, and boiling heat transfer limits of the heat pipe. It was found that the capillary limit leads to the determination of the maximum heat transfer limit. Xin et al. [13] aimed to design the optimum mini grooved flat heat pipe. A mathematical model of axial fluid flow and heat transfer in a mini grooved flat heat pipe has been created. They emphasized that capillary radius values are an important parameter for calculating capillary limit values. Zhou et al. [14] investigated experimentally the effects of ultra-thin heat pipe, wick width, and fill rate parameters on thermal performance. It was found that when the wick width is 4 mm, the maximum heat carrying capacity of the ultra-thin heat pipe can reach 8.5 W. Zhang et al. [15] characterized the porous structures and capillary performances of the wicks and measured the thermal efficiency of the heat pipes to calculate the capillary limit of the heat pipe. Copper powder sintered heat pipes in various shapes, dendritic and irregular powder

heat pipes provided superior heat transfer capabilities. Some researchers work on entrainment limit. Sandeep and Prakash [16] conducted a study on copper heat pipe filling with acetone. The capillary and entrainment limits were investigated. Python code was used for calculating capillary and entrainment limits. The highest values of capillary and entrainment limits were found as 52.6 W and 98.65 W, respectively. Mansour [17] researched the heat convection limits and heat transfer coefficient for a heat pipe using copper-acetone at various vapor temperatures. A new correlation for the heat transfer coefficient was developed. Latent heat evaporation, pipe diameter, and Reynolds number were effective on all heat transfer limits presented. It was observed that while an increment in the capillary, entrainment and capillary limits occurs with the increase in vapor temperature, the boiling limit is reduced.

## THE CONCEPT OF HEAT PIPE

A heat pipe is a mechanism that makes it possible to transport thermal energy efficiently. It consists of a structure whose inner surface is covered with a thin layer of porous material, usually called grooved. The container can be made in a cylindrical shape or in any other suitable shape. The pores of the wick are filled with a working liquid suitable for the application, and the liquid vapor covers the remaining internal volume. Since the vapor and its liquid are in equilibrium, the pressure value in the vessel is same to the vapor pressure value, which conforms with saturation conditions [18].

Heat pipes have a simple configuration and a simple heat transfer mechanism. The heat pipe structure is presented in Fig. 1. Heat pipes allow very efficient heat transfer from one end to the other. When heat is applied on the evaporator part, while the working liquid vaporizes from the wick, it causes the condensation of the vapor on the wick in the condensation part and removes heat by releasing the latent heat of the vapor [18].

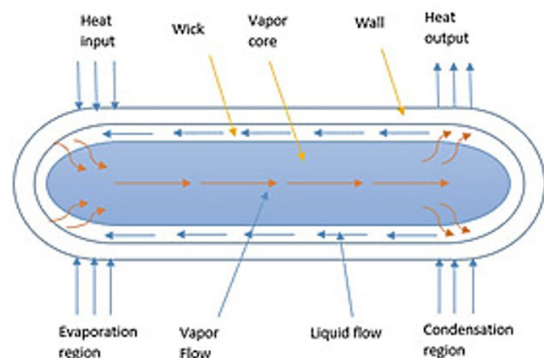


Figure 1. Structure of heat pipe

## Heat Pipe Nuclear Reactors

Reactors require a circulating pump or transport fission or decomposition heat with liquid or gas based on a natural circulation, so the use of heat pipes for primary heat transfer is a new approach. The usage of heat pipes technology for nuclear reactors is new for the nuclear industry. However, heat pipe technology has been researched for decades and numerous tests have been conducted in both radiation and non-radiation test environments.

A heat pipe reactor simplifies system integration. Namely eliminating the components required for a pumped loop. This simplifies the system. Other advantages of using heat pipes in a nuclear reactor include modularity, testability, simplified system integration, passivity, and elimination of single point failures. It has also been suggested that the reactor design can operate for more than 10 years without adding fuel and is best suited to serve as a nuclear battery rather than a central power source [19,20].

In this study, the effects of important parameters affecting the capillary limit, such as porosity radius, wick permeability, and wick radius were investigated in a heat pipe reactor with potassium liquid as working fluid. Besides, the effect of the porous radius was studied for entrainment limit.

## MATERIALS AND METHODS

The dimensions and materials of the potassium liquid heat pipes used in this study were taken from the literature [21] and the sizes of the heat pipes are presented in Table 1.

**Table 1.** Heat Pipe Dimension [21].

Evaporation length	450 mm
Adiabatic length	600 mm
Condenser length	1200 mm
Vapor core radius	18 mm
Wall thickness	30 mm
Wick thickness	26.4 mm

The operating temperature of the heat pipe nuclear reactor which is a hypothetical nuclear power plant was assumed to be 650 K and calculations were made based on 650 K. The potassium working fluid was used following the work of [22, 23] and at the above assumed temperature. Neutron absorption values are also one of the important factors in selecting a material for a nuclear reactor. Potassium is a suitable material for use in nuclear reactors because it has a low neutron absorption cross section.

The most appropriate correlations for the capillary limit were taken from the literature to correctly calculate the heat extraction value in a heat pipe nuclear reactor. The

necessary parameters for the heat pipe calculations were taken from the values given in Table 1. In addition, the thermophysical properties of potassium were calculated using Ref [24-27].

The porosity radius and wick permeability of the sintered copper tube heat pipe were selected and evaluated following the literature [28-31]. Some important parameters affect the capillary limit, such as porosity radius, wick permeability, wick radius, thermophysical properties of the fluid, and contact angle. Five different porosity radius (10.1x10<sup>-6</sup>, 10.225x10<sup>-6</sup>, 10.35x10<sup>-6</sup>, 10.425x10<sup>-6</sup>, and 10.6x10<sup>-6</sup> m) and five different wick permeabilities (4.75x10<sup>-12</sup>, 5x10<sup>-12</sup>, 5.25x10<sup>-11</sup>, 5.5x10<sup>-12</sup>, and 5.75x10<sup>-12</sup> m<sup>2</sup>) were considered and the effects of these parameters on the capillary limit were investigated. In these calculations, the capillary limit was calculated using Eq. (1) and it is given as follow,

$$Q_c = \frac{\sigma L_v \rho_l}{12 \mu_l} \cdot \frac{K A_w}{l_{eff}} \cdot \left( \frac{2}{r_{eff}} - \frac{\rho_l \cdot g \cdot \cos \psi \cdot l_t}{\sigma} \right) \quad (1)$$

In Eq. (1),  $l_v$  is latent heat (J/kg),  $\sigma$  is surface tension (N/m),  $A_w$  is cross-sectional area of wick (m<sup>2</sup>),  $\rho_l$  is density of liquid (kg/m<sup>3</sup>),  $K$  is wick permeability (m<sup>2</sup>),  $\mu_l$  is viscosity of fluid (N-s/m<sup>2</sup>),  $r_{eff}$  effective porosity radius of wick (m),  $g$  is gravitational force (9.8 m/s<sup>2</sup>) and  $l_t$  is total length of heat pipe (m). where  $\psi$  is the contact angle between the liquid and the wick. Here this angle is assumed to be 90°.  $r_{eff}$  is the effective radius of the surface pore (m) and  $K$  (wick permeability) values were taken from ref [28-31] in accordance with the literature.  $l_{eff}$  is the effective length of the heat pipe (m) and is expressed as follows;

$$l_{eff} = \frac{L_{evaporator}}{2} + L_{adiabatic} + \frac{L_{condenser}}{2} \quad (2)$$

where  $L_{evaporator}$  is the evaporation zone length (m), the  $L_{adiabatic}$  is adiabatic zone length (m) and the  $L_{condenser}$  is the condensation zone length (m).

Five different porosity radii (10.1x10<sup>-6</sup>, 10.225x10<sup>-6</sup>, 10.35x10<sup>-6</sup>, 10.425x10<sup>-6</sup>, and 10.6x10<sup>-6</sup> m) were considered and the effects of these parameters on the entrainment limit were investigated. The entrainment limit was calculated by using Eq. (3) The equation is given as follow [28];

$$Q_{sr} = A_v \cdot L_v \cdot \sqrt{\frac{\rho_v \cdot \sigma}{2 r_c}} \quad (3)$$

Here,  $r_c$  is the hydraulic radius of the surface pore (m),  $A_v$  is vapor core cross-sectional area (m<sup>2</sup>) and  $\rho_v$  is vapor

density ( $\text{kg/m}^3$ ). It is assumed that the wick hydraulic radius is equal to the effective of porosity radius for entrainment limit.

All calculations are done by using calculator.

## RESULTS AND DISCUSSION

### Capillary Limit

The capillary limit is related to the fundamental conditions that enable heat pipe operation and is formed due to capillary pressure differentiation at the vapour-liquid interfaces in the section of the evaporator and condenser. The driving potential for liquid circulation is the capillary pressure differentiation, the maximum capillary pressure has to be higher than the sum of all pressure drops in the heat pipe.

The maximum heat transfer rate can be specified because of capillary limitation for most of the heat pipes, [28,32].

### Effect of Porosity Radius on Capillary Limit

The pore radius directly affects the capillary pumping potential, as a smaller pore radius results in higher capillary pressure. Pore size and wick properties affect the operating limits of heat pipes. It has become a popular topic to work on the fabrication of new wicks with improved properties that can hinder the development of vapor in the porous structure or release it easily. Many studies have been conducted on the effects of the properties of the porous structure on heat limitation [32-34].

Fig. 2 demonstrates the variation of the capillary limit with temperature for all effective porosity radii. Eq. (1) is used to calculate the capillary limit. As can be seen from the figure, the capillary limit does not change significantly with

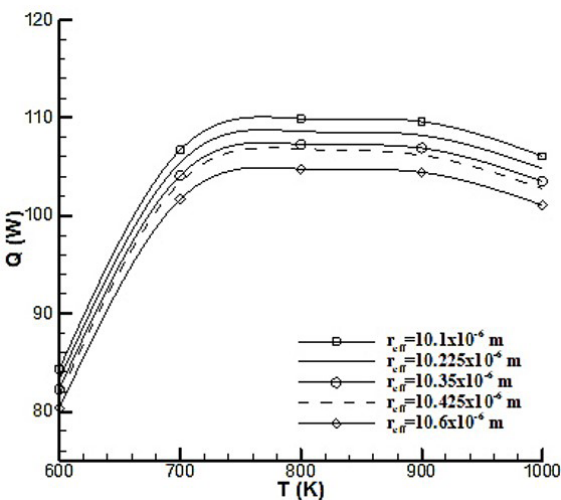


**Figure 2.** The variation of capillary limit with temperature for all effective porosity radius

increasing temperature. The values of capillary limit were calculated when the effective porosity radius was  $10.1 \times 10^{-6}$ ,  $10.225 \times 10^{-6}$ ,  $10.35 \times 10^{-6}$ ,  $10.425 \times 10^{-6}$  and  $10.6 \times 10^{-6}$  m ( $K=4.75 \times 10^{-12} \text{ m}^2$ ). The capillary limit changes inversely with the effective porosity radius. For this reason, the capillary limit values decrease as the effective porosity radius increases. The highest capillary limit values were found the effective porosity radius was  $10.1 \times 10^{-6}$  m, while the lowest capillary limit values were found when the porosity was  $10.6 \times 10^{-6}$  m.

The graph of capillary limits for five different effective porosity radii at a temperature of 650 K is presented in Fig. 3. It can be seen from the Fig. 3, the value of the capillary limit value decreases as the effective porosity radius increases. When the values of effective porosity radius are  $10.1 \times 10^{-6}$ ,  $10.225 \times 10^{-6}$ ,  $10.35 \times 10^{-6}$ ,  $10.425 \times 10^{-6}$  and  $10.6 \times 10^{-6}$  m at a temperature of 650 K, the capillary limit values are 95.5, 94.3, 93.2, 92.5 and 90.8 W, respectively. The highest capillary limits occurred when the effective porosity radius was  $10.1 \times 10^{-6}$  m. Since the effective porosity radius inversely proportional with the capillary limits, the highest capillary limit is obtained when the lowest effective porosity radius is used.

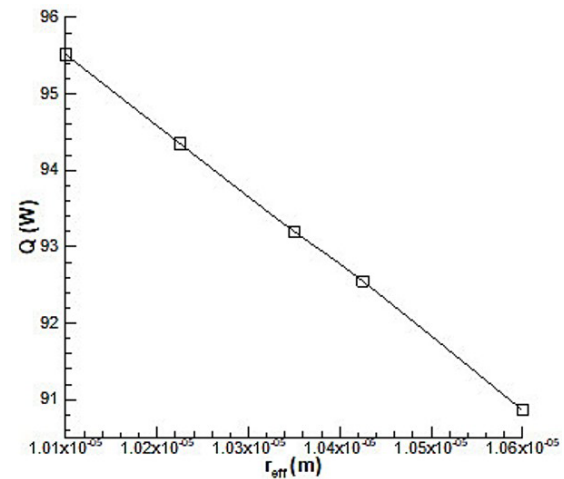


**Figure 3.** Variation of capillary limit values for all porosity radius at a temperature of 650 K.

### Effect of Wick Permeability on Capillary Limit

The increment in the permeability can cause a decrement in flow resistance and increment of the capillary limit. The wick permeability is one of the most significant parameters effecting the capillary limit. The effect of wick permeability on capillary limit is an interesting topic for researchers [35,36].

Fig. 4 shows the change in the effect of wick permeability on the capillary limit with temperature. As can be seen, the capillary limit does not change significantly with incre-

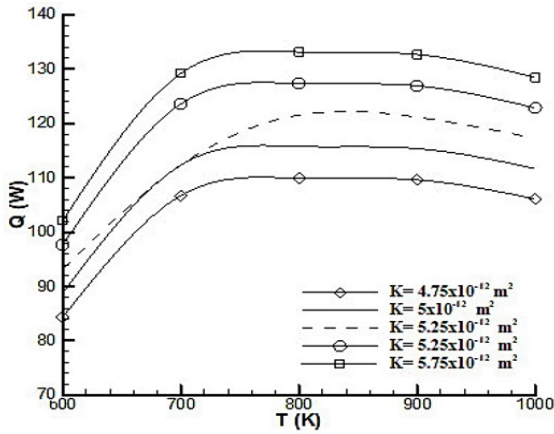


**Figure 4.** Variation of the effect of wick permeability on the capillary limit with temperature

asing temperature. The capillary limit increases with increasing wick permeability. The reason for this is that the wick permeability and the capillary limit are directly proportional. The capillary limits were calculated for wick permeability  $4.75 \times 10^{-12}$ ,  $5 \times 10^{-12}$ ,  $5.25 \times 10^{-11}$ ,  $5.5 \times 10^{-12}$  and  $5.75 \times 10^{-12} \text{ m}^2$  (the porosity radius was assumed to be  $10.1 \times 10^{-6} \text{ m}$ ). The results show that the highest capillary limit is obtained when the wick permeability is  $5.75 \times 10^{-12} \text{ m}^2$ , while the lowest capillary limit is obtained when it is  $4.75 \times 10^{-12} \text{ m}^2$ .

The graph of capillary limits for five different effective wick permeability values at a temperature of 650 K is shown in Fig. 5. The wick permeability is plotted such that the capillary limit value increases with increasing permeability. From Fig. 5, it can be seen that as the permeability increases, the capillary limit value also increases. At 650 K, when the permeability of the wicks is  $4.75 \times 10^{-12}$ ,  $5 \times 10^{-12}$ ,  $5.25 \times 10^{-11}$ ,  $5.5 \times 10^{-12}$  and  $5.75 \times 10^{-12} \text{ m}^2$ , the capillary limit values are 95.5, 100.5, 102.7, 110.6 and 115.6 W, respectively. The case where the capillary limit is the highest is the one where the wick permeability value is  $5.75 \times 10^{-12} \text{ m}^2$ .

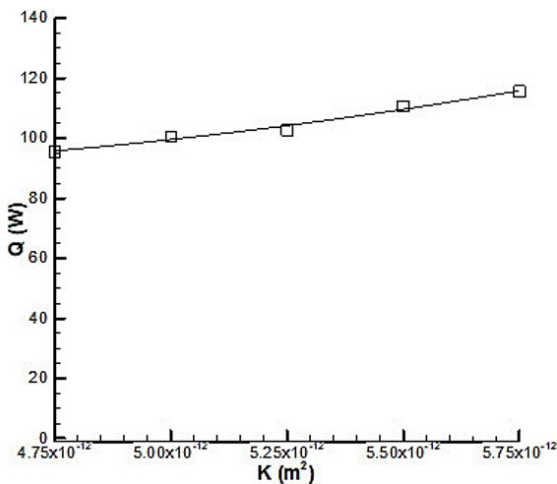


**Figure 5.** Variation of capillary limit values for all wick permeability values at a temperature of 650 K

## Entrainment Limit

Since vapor and liquid move in converse directions, a shear force occurs at the interface between liquid vapor interfaces. At high relative speeds, liquid droplets can break off from the wick surface and enter the vapor flowing into the condensation region. If the entrainment is too much, the evaporation zone dries out. The entrainment limit is the heat transfer rate at which this phenomenon occurs. Entrainment is determined by the sound of droplets hitting the condenser region end of the heat pipe. The entrainment limit is generally associated with either low or medium temperature small diameter heat pipes or heat pipes has high temperature when heat input is high in the evaporator zone. Eq. (3) is used to calculate the entrainment limit.

## Effect of Porosity Radius on Entrainment Limit

Fig. 6 shows the variation of entrainment limit with temperature for all effective porosity radii. Eq. (1) is used in the capillary limit calculations. It can be seen from Fig. 5 that entrainment increases with increasing temperature. The entrainment limits were calculated once the effective porosity radius was  $10.1 \times 10^{-6}$ ,  $10.225 \times 10^{-6}$ ,  $10.35 \times 10^{-6}$ ,  $10.425 \times 10^{-6}$ , and  $10.6 \times 10^{-6} \text{ m}$ . The entrainment limit and the effective porosity radius are inversely proportional. Therefore, the entrainment limits reduce as the effective porosity radius increases. When the effective porosity radius was  $10.1 \times 10^{-6} \text{ m}$ , the highest entrainment limit was achieved.

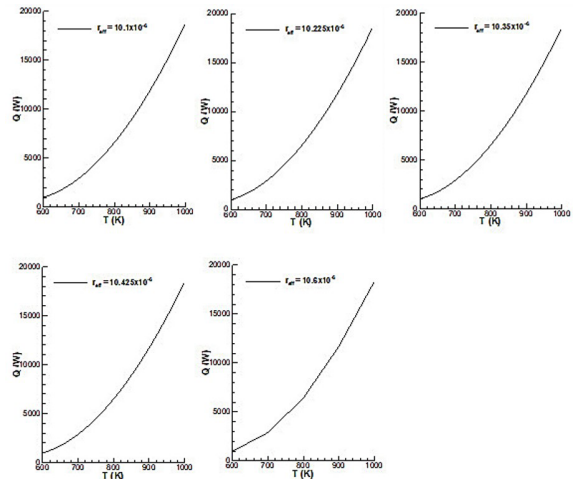


**Figure 6.** Variation of entrainment limit with temperature for all effective porosity radius.

In Fig. 7 entrainment limits for five values of the effective porosity radius at a temperature of 650 K is presented. Increasing the effective porosity radius resulted in decreasing the entrainment limits. At 650 K, when the effective porosity radius is  $10.1 \times 10^{-6}$ ,  $10.225 \times 10^{-6}$ ,  $10.35 \times 10^{-6}$ ,  $10.425 \times 10^{-6}$ , and  $10.6 \times 10^{-6} \text{ m}$ , the entrainment limits are 2310, 1968, 1956,

1949, and 1945 W, respectively. The highest entrainment limit was reached when the effective porosity radius is  $10.1 \times 10^{-6}$  m.

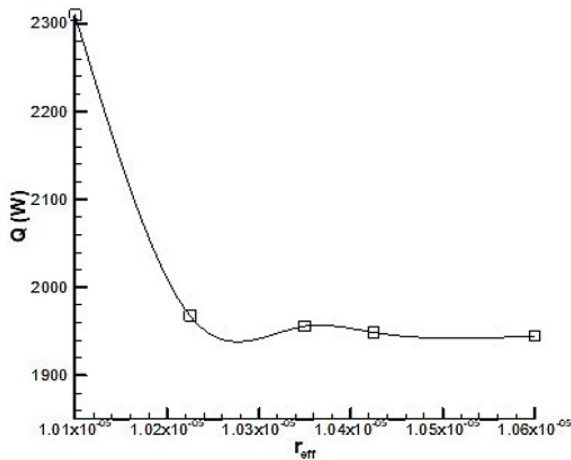


**Figure 7.** Variation of entrainment limit values for all values for all porosity radius at a temperature of 650 K

## CONCLUSION

In this study, the effects of effective porosity radius and wick permeability on capillarity and entrainment limit in a heat pipe nuclear reactor were investigated. Based on the results of this study, the following conclusions are made:

- The highest capillary limit was reached when the effective porosity was  $10.1 \times 10^{-6}$  m.
- A decrease in effective porosity results in an increase in capillary limit
- The case where the capillary limit is obtained highest is when the wick permeability value is  $5.75 \times 10^{-12}$  m<sup>2</sup>.
- An increase in wick permeability results in an increase in capillary limit.
- When the effective porosity radius was  $10.1 \times 10^{-6}$  m, the highest entrainment limit was achieved.
- An decrease in effective porosity results in an increase in entrainment limit.
- It has been found that the capillary limit is more effective than the entrainment limit in determining the heat pipe limitation. This is because the capillary limit has lower temperature values.
- For this heat pipe reactor, the best effective porosity radius and permeability are determined as  $10.1 \times 10^{-6}$  m and  $5.75 \times 10^{-12}$  m<sup>2</sup>, respectively.

## CONFLICT OF INTEREST

The author deny any conflict of interest.

## REFERENCES

1. Wright SA, Lipinski RJ, Pandya T, Peters. Proposed design and operation of a heat pipe

reactor using the Sandia National Laboratories Annular Core test facility and existing UZrH fuel pins. Space Technology and Applications International Forum–Staif. 2005,746; 449–60. doi:10.1063/1.1867161

2. Koenig DR, Ranken WA, Salmi EW. Heat-pipe reactors for space power applications. *Journal of Energy*. 1977, 237–43. doi:10.2514/3.62334
3. Greenspan E. Solid Core Heat-Pipe Nuclear Battery Type Reactor, University of California. 2008. doi:10.2172/940911.
4. Ma Y, Chen E, Yu H, Zhong R, Deng J, Chai X, Huang S, Ding S, Zhang Z. Heat pipe failure accident analysis in megawatt heat pipe cooled reactor. *Annals of Nuclear Energy*. 2020, 149; 107755. doi: 10.1016/j.anucene.2020.107755
5. Sun H, Wang C, Ma P, Tian W, Qiu S, Su G. Conceptual design and analysis of a multipurpose micro nuclear reactor power source. *Annals of Nuclear Energy*. 2018,121; 118–27. doi:10.1016/j.anucene.2018.07.025
6. Zhang W, Zhang D, Liu X, Tian S, Qiu S, Su G. Thermal-hydraulic analysis of the thermoelectric space reactor power system with a potassium heat pipe radiator. *Annals of Nuclear Energy*. 2020, 136;19–25. doi: 10.1016/j.net.2019.06.021
7. Liu X, Sun H, Tang S, Wang C, Tian W, Qiu S, Su G. Thermal - hydraulic design features of a micronuclear reactor power source applied for multipurpose. *International Journal of Energy Research*. 2019, 43; 4170–183. doi: 10.1002/er.4542
8. Wang C, Liu M, Zhang D, Qiu S, Su GH, Tian W. Experimental study on transient performance of heat pipe-cooled passive residual heat removal system of a molten salt reactor. *Progress in Nuclear Energy*. 2020, 118; 103113. doi: 10.1016/j.pnucene.2019.103113
9. Wang C, Sun H, Yang S, et al., Thermal-hydraulic analysis of a new conceptual heat pipe cooled small nuclear reactor system. *Nuclear Engineering and Technology*. 2020, 52; 19–26. doi: 10.1016/j.net.2019.06.021
10. Guilen DP, Turner CG, Assessment of Screen-Covered Grooved Sodium Heat Pipes for Microreactor Applications. *Nuclear Technology*. 2022, 208; 1301–310. doi:10.1080/00295450.2021.1977085.
11. Subedi B, Kim SY, Jang SP, Kedzierski MA. Effect of mesh wick geometry on the maximum heat transfer rate of flat-micro heat pipes with multi-heat sources and sinks. *International Journal of Heat and Mass Transfer*. 2019, 131; 537–45. doi: 10.1016/j.ijheatmasstransfer.2018.11.086
12. Yu M, Diallo TMO, Zhao X, Zhou J, Du Z, Ji J, Chen Y, Analytical study of impact of the wick's fractal parameters on the heat transfer capacity of a novel micro-channel loop heat pipe. *Energy*. 2018, 158; 746–759. Doi: 10.1016/j.energy.2018.06.075
13. Xin F, Ma T, Wang Q, Thermal performance analysis of flat heat pipe with graded mini-grooves wick. *Applied Energy*. 2018, 228; 2129–139. Doi: 10.1016/j.apenergy.2018.07.053

14. Zhou W, Li Y, Chen Z, Effect of the passage area ratio of liquid to vapor on an ultra-thin flattened heat pipe, *Applied Thermal Engineering*. 2019, 162; 114215.
15. Zhang J, Lian L, Liu Y, Wang R, The heat transfer capability prediction of heat pipes based on capillary rise test of wicks. *International Journal of Heat and Mass Transfer*. 2021, 164; 120536. doi: 10.1016/j.ijheatmasstransfer.2020.120536
16. Meseguer J, Perez-Grande I, Sanz-Andrés A. Heat pipes. *Spacecraft Thermal Control*. 2012, 175-207. Doi: 10.1533/9780857096081
17. Sandeep SS, Prakash SB. Design of heat pipe based on capillary and entrainment limitations. *AIP Conference Proceedings*. 2019, 2200(1). Doi: 10.1063/1.5141239
18. Mansour M, Heat Transport Limitations and Overall Heat Transfer Coefficient for a Heat Pipe. *International Journal of Engineering and Advanced Technology (IJEAT)*. 2016, 5(4); 119-23.
19. El-Genk, MS. Space nuclear reactor concepts for avoidance of a single point failure. *Nuclear Energy and Design*. 2008, 238; 2245-255.
20. Yuan Y, Shan JQ, Zhang B, Gou J, Bo Z, Lu T, Ge L, Yang Z. Accident analysis of heat pipe cooled and AMTEC conversion space reactor system. *Annals of Nuclear Energy*. 2016, 94; 706-71. doi: 10.1016/j.anucene.2016.04.017
21. Zhang Y, Guo K, Wang C, Tang S, Zhang D, Tian W, Su GH. Numerical analysis of segmented thermoelectric generators applied in the heat pipe cooled nuclear reactor. *Applied Thermal Engineering*. 2022, 204; 117949. Doi: 10.1016/j.applthermaleng.2021.117949
22. Peterson G. An overview of micro heat pipe research and development. *Journal Applied Mechanics Review*. 1992, 45; 175-189. doi: 10.1115/1.3119755
23. Karabulut K, Alnak DE. Investigation of heat transfer and flow properties in separated flow and reattachment regions for liquid sodium flow at fast reactors. *Nuclear Engineering and Design*. 2021, 379; 1-5. Doi: 10.1016/j.nucengdes.2021.111224
24. Faghri A, Zhang Y. *Transport phenomena in multiphase systems*. Elsevier, Burlington, MA, 2006, 1030.
25. Faghri A, Zhang Y, Howell J, *Advanced heat and mass transfer*. 1st ed., Global Digital Press, Columbia, MO, 2010, 934.
26. Ivanovskii MN, Sorokin VP, Yagodkin IV. *The physical principles of heat pipes*. Clarendon Press, Oxford, United Kingdom, 1982, 268.
27. Vargaftik NB. *Handbook of physical properties of liquids and gases*. Hemisphere, New York, NY, 1975, 758.
28. Chi W. *Heat pipe theory and practice*. Hemisphere Publishing Corporation, New York, 1976, 242.
29. Deng D, Liang D, Tang Y, Evaluation of capillary performance of sintered porous wicks for loop heat pipe. *Experimental Thermal and Fluid Science*. 2013, 50; 1-9. doi: 10.1016/j.expthermflusci.2013.04.014
30. Semenic T, Lin YY, Catton I, Thermophysical properties of biporous heat pipe evaporators, *ASME Journal of Heat Transfer*. 2008, 130; 022602. doi: 10.1115/1.2790020
31. Dominguez Espinosa FA, Peters TB, Brisson JG. Effect of fabrication parameters on the thermophysical properties of sintered wicks for heat pipe applications. *International Journal of Heat Mass Transfer*. 2012, 55; 7471-7486. doi: 10.1016/j.ijheatmasstransfer.2012.07.037
32. Busse CA. Theory of the ultimate transfer of cylindrical heat pipes. *International Journal of Heat and Mass Transfer*. 1973, 16; 169-186. Doi: 10.1016/0017-9310(73)90260-3
33. Ochterbeck JM, *Heat pipes, Heat Transfer Handbook*, 1st ed., 2003, 1481.
34. Williams RR, Harris DK, A device and technique to measure the heat transfer limit of a planar heat pipe wick. *Experimental Thermal and Fluid Science*. 2006, 3; 277-284. Doi: 10.1016/j.expthermflusci.2005.07.008
35. Holley B, Faghri A. Permeability and effective pore radius measurements for heat pipe and fuel cell applications. *Applied Thermal Engineering*. 2006, 26; 448-462. Doi: 10.1016/j.applthermaleng.2005.05.023.
36. Carnogurská M, Píhoda M, Brestovi T, Molínek J, Pyszko R. Determination of permeability and inertial resistance coefficient of filter inserts used in the cleaning of natural gas. *Journal of Mechanical Science and Technology*. 2012, 26; 103-111. Doi: 10.1007/s12206-011-0937-3.